

# In-wheel motor vibration control for distributed-driven electric vehicles

Ze Zhao, Hamid Taghavifar, Haiping Du, Yechen Qin, Mingming Dong, and Liang Gu

**Author post-print (accepted) deposited by Coventry University's Repository**

**Original citation & hyperlink:**

Zhao, Z., Taghavifar, H., Du, H., Qin, Y., Dong, M. and Gu, L., 2021. In-wheel motor vibration control for distributed-driven electric vehicles: A review. *IEEE Transactions on Transportation Electrification*.

<https://dx.doi.org/10.1109/TTE.2021.3074970>

DOI [10.1109/TTE.2021.3074970](https://dx.doi.org/10.1109/TTE.2021.3074970)

ISSN [2332-7782](https://dx.doi.org/10.1109/TTE.2021.3074970)

Publisher: IEEE

**© 2021 IEEE. Personal use of this material is permitted. Permission from IEEE must be obtained for all other uses, in any current or future media, including reprinting/republishing this material for advertising or promotional purposes, creating new collective works, for resale or redistribution to servers or lists, or reuse of any copyrighted component of this work in other works.**

**Copyright © and Moral Rights are retained by the author(s) and/ or other copyright owners. A copy can be downloaded for personal non-commercial research or study, without prior permission or charge. This item cannot be reproduced or quoted extensively from without first obtaining permission in writing from the copyright holder(s). The content must not be changed in any way or sold commercially in any format or medium without the formal permission of the copyright holders.**

**This document is the author's post-print version, incorporating any revisions agreed during the peer-review process. Some differences between the published version and this version may remain and you are advised to consult the published version if you wish to cite from it.**

## In-wheel motor vibration control for distributed-driven electric vehicles: A review

Ze Zhao, Hamid Taghavifar (Member, IEEE), Haiping Du (Senior Member, IEEE), Yechen Qin\* (Member, IEEE),

Mingming Dong (Member, IEEE), and Liang Gu

**Abstract**—Efficient, safe, and comfortable electric vehicles (EVs) are essential for the creation of a sustainable transport system. Distributed-driven EVs, which often use in-wheel motors (IWMs), have many benefits with respect to size (compactness), controllability, and efficiency. However, the vibration of IWMs is a particularly important factor for both passengers and drivers, and it is therefore crucial for a successful commercialization of distributed-driven EVs. This paper provides a comprehensive literature review and state-of-the-art vibration-source-analysis and -mitigation methods in IWMs. First, selection criteria are given for IWMs, and a multidimensional comparison for several motor types is provided. The IWM vibration sources are then divided into internally-, and externally-induced vibration sources and discussed in detail. Next, vibration reduction methods, which include motor-structure optimization, motor controller, and additional control-components, are reviewed. Emerging research trends and an outlook for future improvement aims are summarized at the end of the paper. This paper can provide useful information for researchers, who are interested in the application and vibration mitigation of IWMs or similar topics.

### Nomenclature

<i>AVC</i>	Active Vibration Cancellation
<i>BLDC</i>	Brushless DC electric motor
<i>CCC</i>	Control of Current Chopping
<i>DVAS</i>	Dynamic Vibration Absorbing Structure
<i>EMF</i>	Electromagnetic Force
<i>EVs</i>	Electric Vehicles
<i>IM</i>	Induction Motor
<i>IWM</i>	In-wheel Motor
<i>NVH</i>	Noise, Vibration, and Harshness
<i>PM</i>	Permanent Magnet
<i>PMSM</i>	Permanent Magnet Synchronous Motor
<i>PWM</i>	Pulse-Width Modulation
<i>RG</i>	Road Grade
<i>RT</i>	Road Type

\*This work was supported in part by the National Science Foundation of China under Grant 51805028, the Beijing Institute of Technology Research Fund Program for Young Scholars and the Young Elite Scientists Sponsorship Program funded by the China Society of Automotive Engineers.

Ze Zhao, Yechen Qin, Mingming Dong and Liang Gu are with School of Mechanical Engineering, Beijing Institute of Technology, Beijing, 100081, China (e-mail: 18458229991@163.com, qinyechenbit@gmail.com, vdm@bit.edu.cn, and guliang@bit.edu.cn).

Yechen Qin is also with Institute of advanced technology, Beijing Institute of Technology, Jinan, 250101, China.

Hamid Taghavifar is with School of Mechanical Aerospace and Automotive Engineering, Coventry University, U.K. (e-mail: ad3380@coventry.ac.uk).

Haiping Du is with School of Electrical, Computer & Telecommunication Engineering, University of Wollongong, Australia. (e-mail: hdu@uow.edu.au).

<i>SRM</i>	Switched Reluctance Motor
<i>UEMF</i>	Unbalanced Electromagnetic Force
<i>V</i>	Velocity
<i>VL</i>	Vertical Load

### I. INTRODUCTION

To reduce the impact of climate change and decreasing fossil-fuel resources, it is highly desirable to make personal and commercial transport more sustainable [1]. New propulsion systems may reduce CO<sub>2</sub> emission and improve energy efficiency, which is of high interest to automobile manufacturers and consumers [2]. Electric vehicles (EVs), in particular, continue to represent a promising alternative type of transport. EVs can be categorized into the following two types, which are based on the number of motors and their configuration: centrally-driven and distributed-driven [3]. Compared to the former type, the distributed-driven EVs, where in-wheel motors (IWMs) are (often) used, have several advantages: a shorter delay-time, better controllability, a more flexible structure, and less cramped chassis space (by omitting the transmission shaft, differential, and speed reducer) [4-6]. For these reasons, this review focuses on IWM of distributed-driven EVs. Furthermore, the rapid advances in motor technology contribute to a wider application of IWMs [7, 8]. However, the increasing expectations for improvements of noise-, vibration-, and harshness- (NVH) performance by consumers make a more in-depth investigation of the NVH characteristics of IWM-driven EVs a highly desirable task [9, 10].

Many published studies focus on the NVH performance of motors. However, a certain amount of vibration due to electro-mechanical/magnetic coupling is inevitable during torque generation because the main function of a motor is to convert electric power into mechanical propulsion power [11, 12]. While the torque ripple, which causes high-frequency vibration, has been studied in depth and is well understood, both system-optimization and control-strategies can only help reduce vibration but never eliminate it completely [13]. Before 2010, the vast majority of studies focused on motor vibration itself, and important improvements were made with respect to the vibration mechanism and optimization. After 2010, with the increasing popularity of electric vehicles, more specific research of motor design, control, and vibration reduction in the electric vehicles' working environment began to appear. Among which, the internally-induced vibration in IWMs attracts more attention. It can be divided into three types: mechanical, aerodynamic, electromagnetic [14]. Among these, electromagnetic vibration is the strongest contributor [15] and mostly affected by a distorted air-gap flux-density distribution [16]. While radial force is the main factor, the vibration due to a large radial force and eccentricity is high [17]. Mechanical vibration is mainly caused by manufacturing imprecision and mechanical anomalies [18, 19]. For aerodynamic vibration,

the cooling system is generally viewed as the main cause [20].

Other than the internally-induced vibration, NVH problems of the vehicle system are widely-studied and continue to be of high interest and importance [21, 22]. However, studies of the vibration-coupling effect of vehicles and IWMs are rare. IWMs helped traditional suspension systems to evolve into IWMs-suspension coupling systems, which should (simultaneously) satisfy the requirements for vibration mitigation and propulsion [23]. The challenging operating environment of IWMs is largely determined by road-induced vehicle vibration, which causes the increased unsprung mass-load to increase suspension vibration [24]. Several studies of IWM-suspension systems were carried out in recent years. In [25], the effect of vehicle speed on vertical vehicle-vibration was studied. The vertical load effect on coupled vertical-longitudinal vibration was discussed in [26]. Furthermore, when the IWMs electro-mechanical-magnetic coupling dynamics are considered, the unbalanced electromagnetic force (UEMF), which is induced by the air-gap vibration, was modelled and its effect on vehicle dynamics was investigated [27]. In addition, a large number of studies focused on the vibration reduction for IWM-suspension systems, such as motor-structure optimization, controller development, and the application of controllable suspension-components [23, 28-30]. Currently, most of such research is based on finite element method and numerical simulation, and the adoption of a simplified vehicle model leaves the comprehensive description of the coupling effect between IWM and vehicle an open question.

Recently, several reviews were carried out to investigate vehicle NVH- [31] and motor- NVH performance [32]. However, a comprehensive literature survey of IWM vibration and its dynamic coupling effect with EVs does not exist. This review aims to fill this gap by providing a comprehensive review of state-of-the-art studies of IWM vibration with respect to IWM modelling, internally- and externally-induced vibration, IWM-vehicle-coupling effect, and control strategies.

This review is organized as follows: Section II introduces the IWM selection and provides a multidimensional comparison for commercially available IWM types. Section III focuses on IWM dynamic modeling and the electro-mechanical/magnetic coupling effect. Section IV analyzes the IWM vibration sources. Section V concludes discusses the various suppression methods that can mitigate vibration in IWMs. Section VI outlines future projects and trends, and the conclusions are summarized in Section VII.

## II. IN-WHEEL-MOTOR MODELLING AND COMPARISON

With respect to their structure, IWMs can be divided into structures with inner rotor and outer rotors. Furthermore, depending on the type of the magnetic field of the motor, they can be categorized into those using radial magnetic fields and those with axial magnetic field [33]. However, perhaps the most practical categorization criterium is to classify according to the type of motor used by the IWMs. An IWM represents an electric propulsion system, where multiple motor types can be used to power wheels. Advances in motor

development with improved power and torque density make the following motors potentially suitable for mass-produced vehicles: brushed motors, brushless DC motors (BLDCs), permanent magnet synchronous motors (PMSMs), switched reluctance motors (SRMs), and induction motors (IMs) [34]. This section introduces motor selection criteria and offers a multidimensional comparison between the different motor types.

### A. Motor selection

Although the automotive industry has been looking for the best suitable motor for mass-produced EVs for IWM-driven EVs, several challenges remain. One major problem is that the motors need to operate within a wide speed-range and meet the demanding driver expectations, vehicle performance requirement, and dimensional constraints. A more detailed requirement list for traction motors is summarized in Fig. 1.

### B. Motor comparison

A multidimensional comprehensive comparison of the above-mentioned motors is given in Table 1, where the advantages, disadvantages, and a score sheet are shown. Note that the investigated motors in Table 1 represent the most representative types that have been used in recent decades. The score sheet, however, only provides a qualitative evaluation of these motors. There are variations for each type, which may show differences with respect to dynamic and NVH performance. For example, surface permanent magnets and internal permanent magnets will be included in PMSMs [35, 36].

According to Table 1, the brushed motor has the lowest score due to its bulky construction, poor efficiency, and power density. In addition, the periodic maintenance requirement also makes it unsuitable for EV propulsion systems [39, 41]. The other four motor types have more balanced advantages and disadvantages, and their scores are very similar. Generally, the usage of permanent magnets (PMs) may be a problem for both BLDCs and PMSMs, for two reasons: 1) Demagnetization can be caused by mechanical pressure or via the stator current when strong

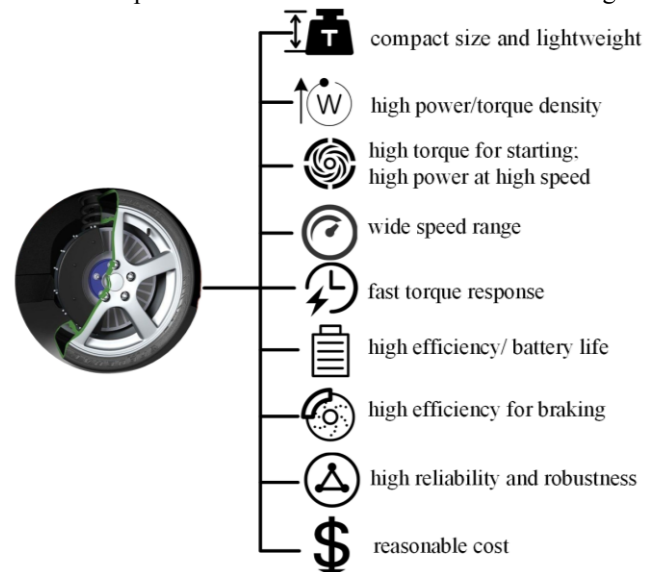
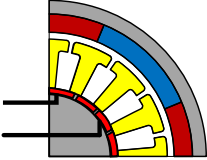
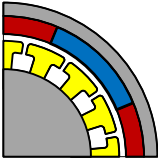
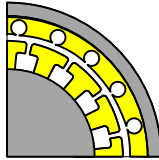
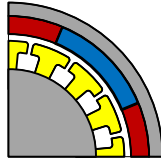
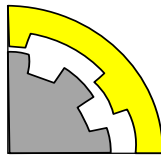


Fig. 1. Requirements for traction motors [36-38].

Table 1. Comparison of different motor types for IWM-driven EVs.

Comparison	Brushed motor	BLDC	IM	PMSM	SRM
√Advantage	<ul style="list-style-type: none"> <li>·Simple control</li> <li>·High starting torque</li> </ul> <i>Refs. [39]</i>	<ul style="list-style-type: none"> <li>·High efficiency</li> <li>·Durability</li> <li>·Simple control</li> <li>·Low weight</li> <li>·Compact construction</li> </ul> <i>Refs. [40]</i>	<ul style="list-style-type: none"> <li>·Robustness</li> <li>·Low price</li> <li>·Mature technology</li> <li>·low maintenance</li> <li>·Wide speed-range</li> </ul> <i>Refs. [39, 41]</i>	<ul style="list-style-type: none"> <li>·High power-density</li> <li>High efficiency</li> <li>High torque/inertia ratio</li> </ul> <i>Refs. [35, 42]</i>	<ul style="list-style-type: none"> <li>·Simple structure</li> <li>·Robustness</li> <li>·Low cost</li> <li>·W/o PM</li> <li>·Wide speed range</li> <li>Easy cooling</li> </ul> <i>Refs. [20, 37, 43]</i>
×Disadvantage	<ul style="list-style-type: none"> <li>·Periodic maintenance</li> <li>·Insufficient propulsion</li> </ul> <i>Refs. [39, 44]</i>	<ul style="list-style-type: none"> <li>·Usage of PM</li> <li>Cogging torque</li> <li>·Demagnetization faults</li> </ul> <i>Refs.[45]</i>	<ul style="list-style-type: none"> <li>Lower torque-density and efficiency</li> <li>high rotor losses</li> </ul> <i>Refs. [36, 46]</i>	<ul style="list-style-type: none"> <li>Usage of PM</li> <li>Cogging torque</li> <li>·Demagnetization faults</li> </ul> <i>Refs. [35, 39, 47]</i>	<ul style="list-style-type: none"> <li>Severe torque ripple;</li> <li>Poor power factor</li> </ul> <i>Refs. [36, 43]</i>
Score (5-best) <i>Refs.</i> [11, 39, 48-50]					
Efficiency	2	4	4	5	4
Weight	2	4	4	4.5	5
Power density	2.5	4	3.5	5	3.5
Controllability	5	4	5	4	3
Reliability	3	4	5	4	5
Maturity	5	5	5	4	4
Cost	4	4	5	3	4
Overall NVH	3	4.5	4	5	3
<b>Σtotal</b>	26.5	33.5	35.5	34.5	31.5

Clearly, the IWMs have drawn more attention in recent years, which led to a significant improvement in both power and torque density – especially within the last 5 years. Note that PMSMs dominate the market due to its electric properties, while Tesla, which is well-known for the application of IMs in their Model-S, began to use PMSM in their new Model-3. The improvement of both power and

Because the shortcomings of the brushed motor are very clear, the rest of this review will focus on the other four motor types and their application in EVs.

The IWMs determine the EVs' propulsion characteristics, and their NVH-dynamics largely determine the IWM-driven EV NVH performance [56]. In addition, the larger runout, which is caused by both internally-induced vibration and externally-induced vibration, generates a radial displacement between stator and rotor in the electric motor. This reduces the performance and the life span of the IWMs [57]. The proportion of vibration of each part of the traditional vehicles and EVs is summarized in Fig. 3 [58]. The figure shows that internal combustion engine vibration and transmission-system vibration dominate at low speed. Generally, IWM vibrations can be categorized into two types: internally-induced vibration and externally-induced vibration [59].

The IWM is a multi-field-coupled system, and its internal vibration is caused by the electromagnetic coupling effect, which can be subdivided into electromagnetic vibration, mechanical vibration, and aerodynamic vibration [14]. Among these categories, electromagnetic vibration is regarded as most significant factor [15].

Electromagnetic forces generate the electromagnetic vibration of motors. They are determined by the flux distribution in the air-gap [28]. Hence, the electromagnetic

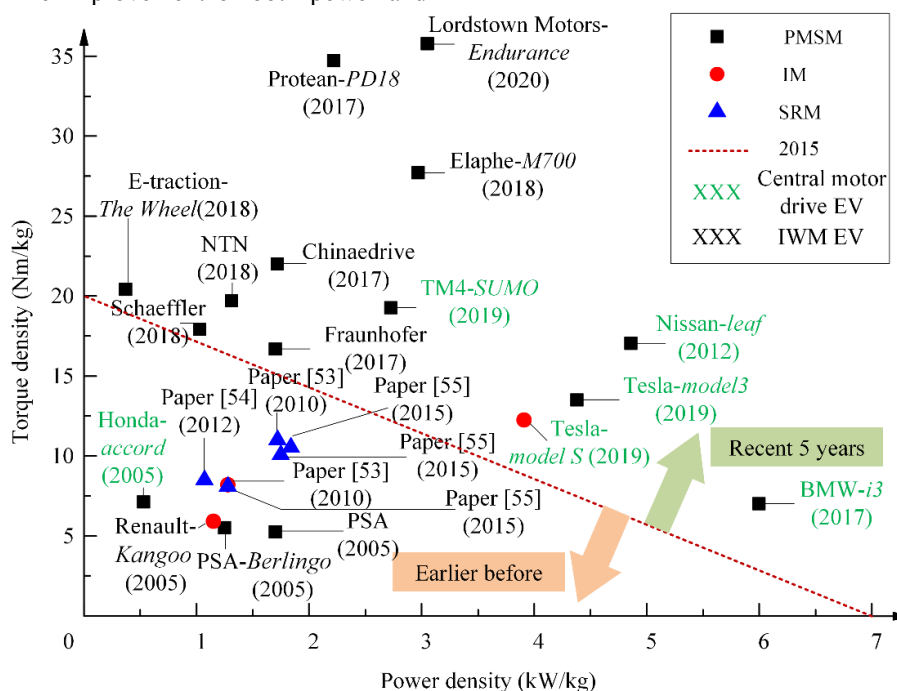


Fig. 2. Comparison of mass-produced motors and commercially-available motors for EVs based on published studies of the past 15 years [53-55].

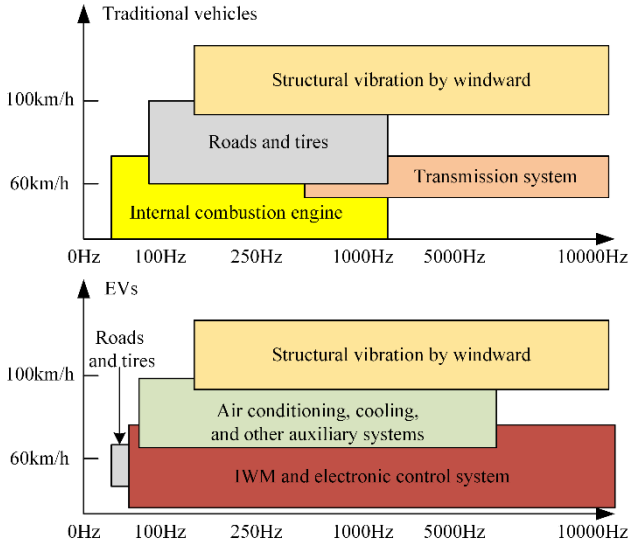


Fig. 3. Distribution of vibration problems of traditional vehicles and EVs.

dynamics are affected by any factor that alters the magnetic field in the air-gap, including the method of excitation and machine geometry [16]. This review describes the electromagnetic force models of all four kinds of motors and summarizes the electromagnetic vibration sources of four types of motors. It then explores the key factors that determine the dynamic characteristics.

To study the vibration caused by electromagnetic force in a motor, it is necessary to know the time and space distribution of the air-gap flux density [60] because the radial and tangential components of the electromagnetic force depend on the radial and tangential components of the flux density. In other words, to accurately predict the electromagnetic vibration, the two components of the air-gap flux density must be determined in the time and space domain [61]. A flow chart for the calculation of the electromagnetic vibration of the motor is shown in Fig. 4.

Three motor-modelling methods are commonly used to calculate the electromagnetic force and vibration, including numerical method, analytical method and semi-analytical method [62]. The numerical method is unable to predict the vibration over a wide speed range and it consumes more time for analysis [63]. The analytical method has relatively low precision, especially for motors with complex structures, significant errors could be produced. Hence, it is common to combine the two previous methods, which is named as semi-analytical method. It calculates the electromagnetic force and derives the vibration via the numerical and analytical method, respectively [64]. Up to now, in the analytical part, the excitations and vibrations can be accurately illustrated via finite element analysis software. The numerical part has been employed in plenty of research, which is elaborately introduced in this section. A commonly used method is Maxwell's stress theory, which uses a microscopic perspective to calculate electromagnetic vibrations [65]. This method assumes that the magnetic-field strength between objects in a vacuum generates stress on the objects' surface, which can be described as [66]:

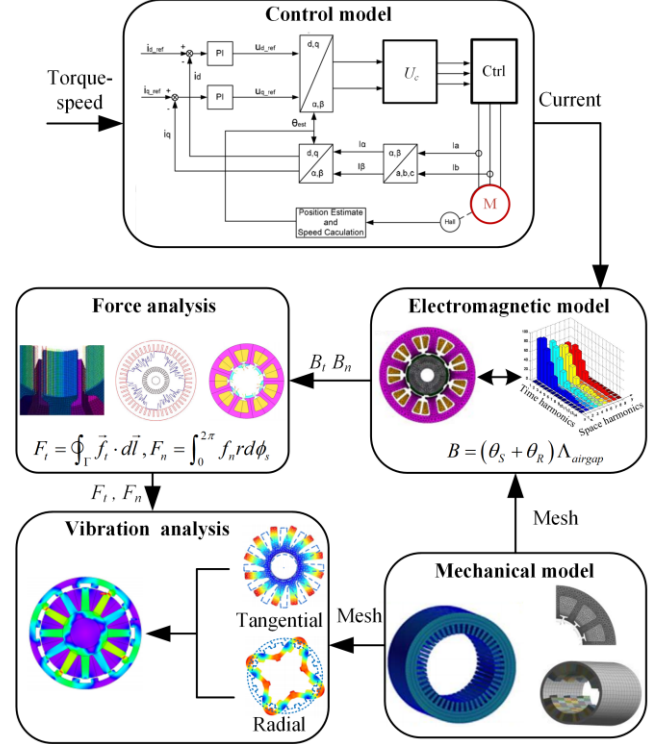


Fig. 4. Flow chart for the calculation of electromagnetic vibration.

$$\begin{cases} B = (\theta_s + \theta_r) \Lambda_{air-gap} \\ f_t = B_n B_t / \mu_0 \\ f_n = (B_n^2 - B_t^2) / 2\mu_0 \\ F_t = \oint_{\Gamma} \vec{f}_t \cdot d\vec{l} \\ F_n = \int_0^{2\pi} f_n r d\phi_s \end{cases} \quad (1)$$

Here,  $\theta_s$  and  $\theta_r$  are the stator- and rotor-armature reaction fields, respectively.  $\Lambda_{air-gap}$  is the real part of the relative permeance [67].  $B_t$  and  $B_n$  represent the tangential and normal components of the flux density in the air gap, and  $\mu_0$  is the permeability of air.  $\Gamma$  is the integration contour in the air-gap.  $r$  is the radius of the integration contour.  $F_t$  and  $F_n$  denote the tangential and radial forces created by the magnetic field strength. When the phases of the motor are energized, a magnetic field is produced due to the current excitation. The magnetic flux generated in the air-gap produces electromagnetic nodal forces that act on the rotor and stator poles [68] – see Fig. 5. The tangential component of the nodal force produces torque on the rotor, while the radial component stretches and compresses the stator [65].

Since the magnetic permeability of the air gap is much lower than the ferromagnetic material, flux lines approximately enter the air gap in radial direction [69]. Therefore, the radial component of flux density is greater than the tangential component, which leads to  $B_n \gg B_t$  [65]. This is also verified by actual calculations and experiments [66, 70, 71]. More specifically, the radial force is about 17

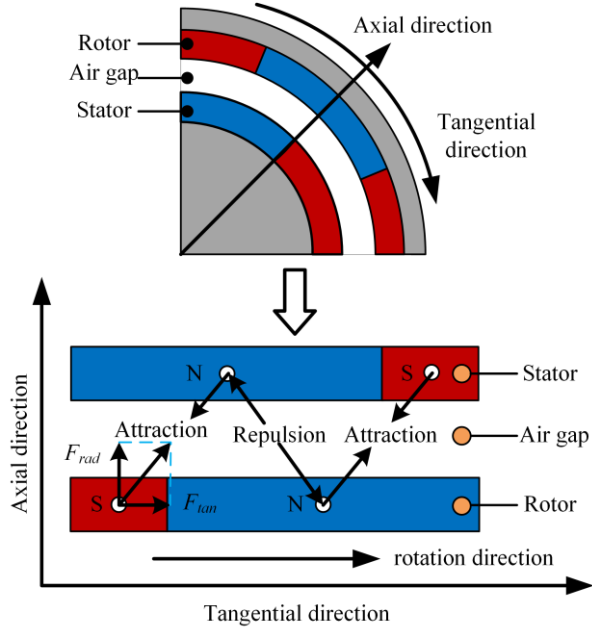


Fig. 5. Electromagnetic forces in a motor.

times higher than the tangential force in an SRM [70], 33 times higher than in an PMSM/BLDC [71], and 49 times higher in an IM [66]. That means rotor- and stator-eccentricity can produce a large radial force and severe vibration. Hence, eccentricity is the main source of electromagnetic vibration among the four motors types. Eccentricity can be divided into two types: static and dynamic. Static eccentricity represents a time-invariant radial air-gap, which is caused by an oval shape or an incorrectly positioned stator core [72]. Dynamic eccentricity is a condition, where the position of the minimum radial air-gap rotates with the rotor. This is caused by worn bearings, curved shafts, asymmetric thermal expansion of the rotor, or high levels of static eccentricity [73].

Eccentricity causes a UEMF, which causes the motor structure and the motor to vibrate [74] - see Fig. 6. UEMF, which is caused by rotor eccentricity, generates a negative stiffness with respect to nonlinearity, which plays a key role in the dynamic behavior [75]. Furthermore, abnormal rotation, induced by mass imbalance and external forces, results in rotor eccentricity, and the UEMF causes the rotor to further move toward the stator and alters the air-gap

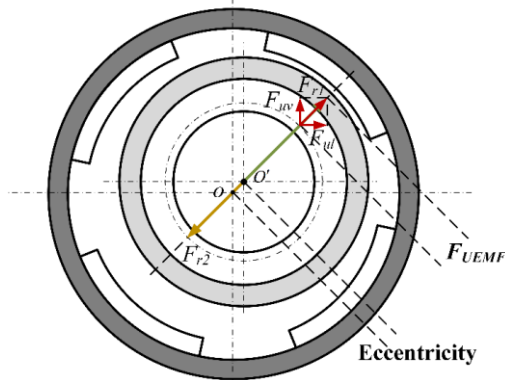


Fig. 6. UEMF analysis.

distribution [76]. These interactions form a typical electromechanical coupling system [77].

However, differences in mechanism, structure, driving mode, and control mechanism affect the electromagnetic properties of the motor systems and result in different vibration characteristics. The electromagnetic vibration sources for the four motor types are listed in the Fig. 7. A more detailed summary of the electromagnetic vibrations of the different motor types is given below:

- *Switched reluctance motors*

SRMs produce torque via the tendency of their rotors to move to a position where the inductance of the excitation winding is maximized. The variability of the reluctance of the magnetic flux is triggered by currents flowing through the stator windings [89]. The best feature of SRMs is that they are not equipped with permanent magnets.

For radial forces, the double salient/pole structure, together with the magnetic saturation characteristic, result in a bigger radial force [98]. The radial force is the main source of motor vibration and is highest near the aligned position. This is because (at the aligned position) nearly all of the flux is concentrated in the radial direction [90], which produces the periodic vibration of the motor.

- *PMSMs and BLDCs*

PMSMs and BLDCs are widely used because of their high potential torque, compactness, and high efficiency. The fundamental difference between them, however, is the difference in excitation current. BLDCs use a trapezoidal excitation current, while PMSMs use sinusoidal currents [11]. Both BLDCs and PMSMs are equipped with permanent magnets and interact with the armature reaction field to generate torque [11, 91]. The driving current, on the other hand, is synchronized based on the rotor-position feedback. As a result, the high similarity with respect to structure and control makes it possible to combine PMSMs and BLDCs into one group for the purpose of modeling [92].

The cogging torque is a special source of vibration in BLDCs/PMSMs [93]. Because of the tooth geometry, the rotor tends to move to certain positions where the effective permeance reaches a maximum. The cogging torque is generated, when the rotor moves [32]. For the other two sources, radial force is regarded as the main cause of vibration in permanent-magnet machines [15]. Furthermore, the radial force frequency is determined by the coupling between the permanent magnetic field and the armature reaction field, when the motor is loaded. The amplitudes are related to the magnet-pole shape as well as the tooth shape [80]. Ripple torque is caused by the abundant harmonics in the magnetic field [15].

- *IMs*

The radial force plays a dominant role in IM vibration. Time harmonics, which are excited by currents in air gap, have a significant effect on the radial force, which is caused by the frequent change of both the starting voltage and the dead-time effect [94]. Furthermore, the 5<sup>th</sup> and 7<sup>th</sup> high time harmonics exert the greatest effect on the radial force [94]. For the torque ripple, the discrete structure of the IM stator slot and the squirrel cage rotor also lead to voltage and current distortion. This alters the magnetic field, produces

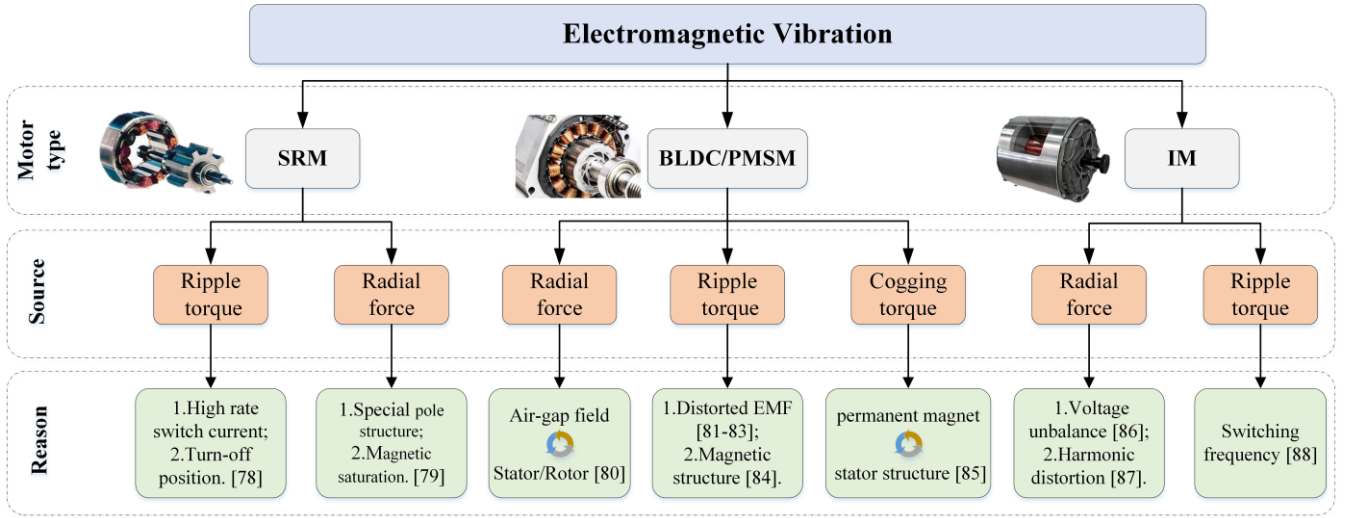


Fig. 7. Sources for electromagnetic vibrations in the four motor types [78-88].

torque motion, and induces torque ripple [95].

## 2. Mechanical and aerodynamic vibration

The main sources of mechanical vibration include manufacturing imprecision and mechanical anomalies [19]. The main source of aerodynamic vibrations is the air flow generated by the cooling fan or a pump [96]. The mechanical and aerodynamic vibrations are summarized in Fig. 8.

- **SRM:** Due to the salient pole structure and placement too close to the coil, the axial force distribution around the circumference of the motor is unfavorable [97], and the structural vibration is severe.
- **PMSM/BLDC:** The asymmetry in the EMF waveform, which is caused by the squared-off shape of the stator lamination and the nonuniform stator-yoke section [81], leads to mechanical vibration.
- **IM:** The mass of the mechanical system and the behavior of the induction machine rotor generate strong inter-coupling, which dominates the overall

vibration of the motor [98].

Resonance frequency and torsional vibration are important for mechanical vibration. Resonance occurs when the main natural frequencies of the structure are excited [99], and higher frequency harmonics lead to resonance at typical speeds (50~100 Hz [100]) [80]. Torsional vibration, which is mainly caused by rotational, repeated, cyclic stresses, varies between tension and compression [101]. In addition, the power supply, the line starting, mechanical imperfections, and load torque pulsation can also induce torsional vibration [18].

The air, water (or oil) cooling systems of the machines are the major sources for the aerodynamic vibration in all motors.

## B. Externally-induced vibration

The use of IWMs upgrades traditional suspension to novel IWM-suspension system, with the functions of added propulsion and vibration reduction [23]. Inside the wheel hub, IWMs operate in high-vibration environments because only

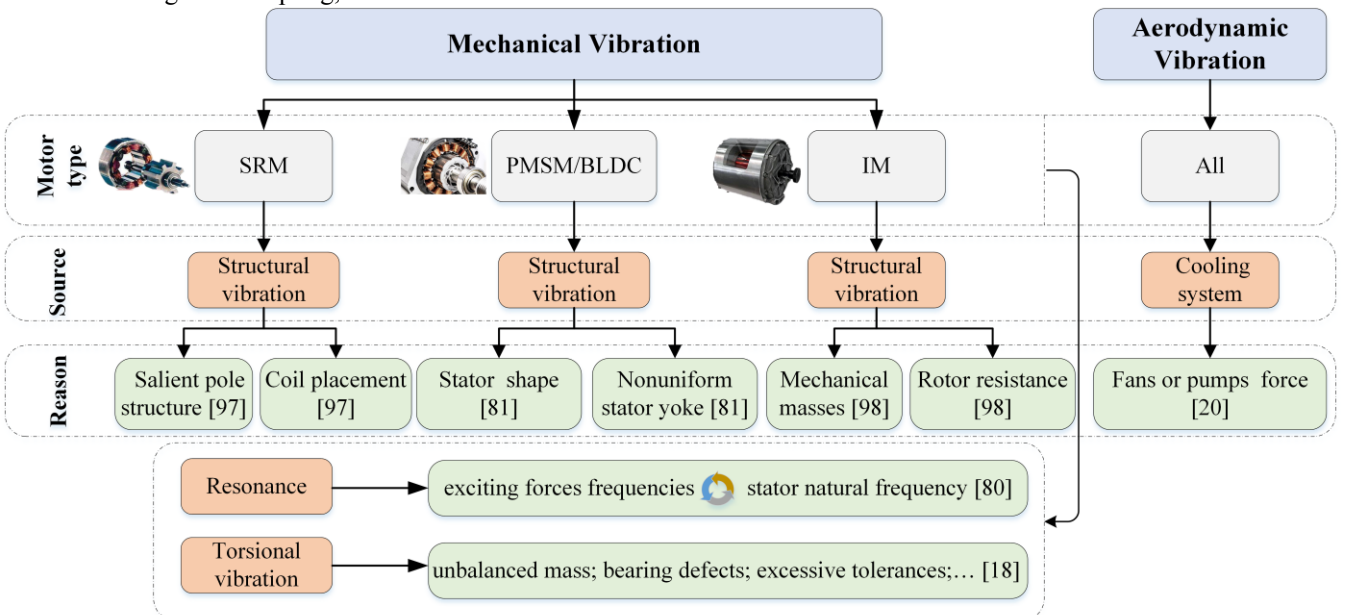


Fig. 8. Mechanical and aerodynamic vibration-sources, and an analysis of their origin [18, 20, 80, 81, 97, 98].

a small portion of road-induced high-frequency vibration can be attenuated by a tire with high radial stiffness. Such external-induced vibration results in time-varying dynamic eccentricity, which causes both electromagnetic and mechanical vibration.

This eccentricity differs from both the static and the dynamic eccentricity discussed in Section III (A), because it is the dynamic response to the interaction between IWM bushing and time-varying road-induced vibration. Thus, both suspension dynamics and road profile characteristics are important for such externally-induced vibration, and numerous studies have been performed in the last 5 years in this field [24]. The longitudinal-vertical coupling IWM-suspension system-dynamics are illustrated in Fig. 9. The IWM-suspension system is dynamically-coupled in longitudinal and vertical direction.

From the vertical perspective, the road grade ( $RG$ ) acts as external excitation [25], which results in vibration for both suspension and IWM at a certain velocity ( $V$ ). The IWM-suspension system transmits the vertical vibration to the IWM, which produces an IWM  $\varepsilon_y$  (time-varying dynamic eccentricity) and induces the  $F_{uv}$ . It can be seen that for the vertical external input,  $RG$  and  $V$  directly affect the response of the vertical vibration, which is similar to conventional vehicles.

With respect to the longitudinal dynamics, the IWM

generates driving torque to balance air-drag and rolling resistance. Road type ( $RT$ ) and vertical load ( $VL$ ) act as the inputs [102], and the difference between wheel speed and vehicle corner speed produces slip-ratio changes [23]. For different  $RT$ ,  $VL$ , and slip ratios, the longitudinal force, which is generated by tires directly, affects  $V$  [103] and transmits a longitudinal  $\varepsilon_x$  to the IWM, inducing a force  $F_{ul}$  [104]. According to the relationship mentioned above, it is clear that the longitudinal response is mainly affected by  $VL$  and  $RT$ .

The big problem that EVs, which are equipped with IWMs, need to overcome is the high vibration environment, where the motor is installed. This condition causes substantial electro-mechanical-magnetic coupling effects [23, 105]. Specifically, the vertical and longitudinal vibration of the suspension transmit to the IWM and produce the time-varying dynamic eccentricity described by  $\varepsilon_x$  and  $\varepsilon_y$ .

According to [23], the air-gap affects the UEMF significantly. For the air-gap variation  $\vec{\varepsilon} = \vec{\varepsilon}_x + \vec{\varepsilon}_y$ , the UEMF  $\vec{F}_r = \vec{F}_{ul} + \vec{F}_{uv}$  shows time-varying dynamics. Because of the internal excitation of the IWM-suspension system, the UEMF further degrades the vibration response of the vehicle suspension. Overall, electro-mechanical-magnetic coupling leads to the deterioration of both ride comfort and handling

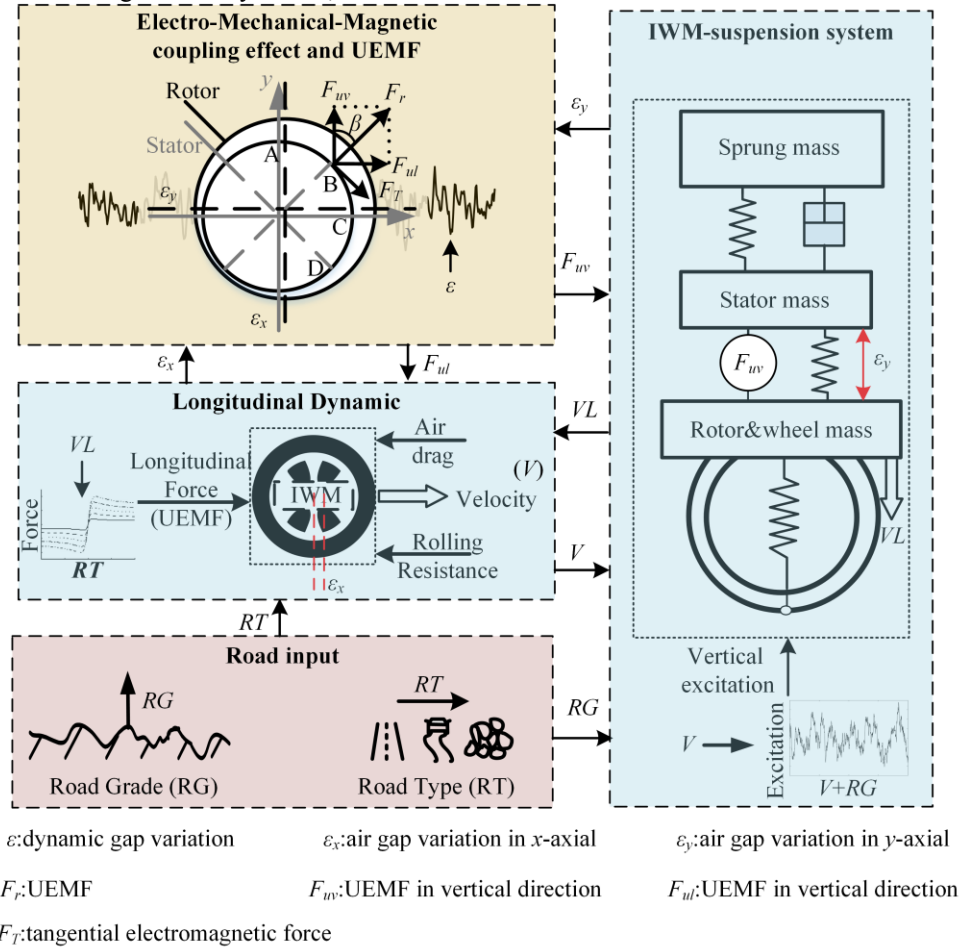


Fig. 9. Longitudinal and vertical dynamics, and the coupling effect in an IWM-suspension system.

performance of the vehicles [24].

#### IV. VIBRATION REDUCTION IN IWM

This section describes the state-of-the-art research related to IWM vibration mitigation. Generally, mechanical vibration and aerodynamic vibration can be optimized relatively easily and as a result contribute only a small proportion to the vibrations in IWMs [106]. For this reason, electromagnetic vibration reduction will be the focus of this section. The methods to reduce electromagnetic vibration include the following three categories: electric motor structure optimization, controller improvements, extra suspension components application.

##### A. Electric motor structural optimization

A useful structural optimization-algorithm can be found by altering the rotor and stator geometries or the windings to minimize the flux-density harmonics [28]. Eq. (1) shows that the non-ideal  $B_t$  and  $B_n$  directly affect the vibration of the motor [107]. Here we summarize the most frequently optimized structural parameters for electric motors of PMSMs/BLDCs - see Table 2.

It can be seen that the torque fluctuation can be significantly optimized via structural optimization. Furthermore, the optimization of the motor structure involves increasing the efficiency, torque density, and the generation of a low torque ripple for a wide range of constant power, which makes the optimization process rather challenging [108]. This represents a multi- objective optimization problem with multiple constraints. For instance, the reduction of the cogging torque using teeth notching schemes often decreases torque density [109]. Therefore, these objectives should be considered as a whole when optimizing.

The above mentioned structural parameters can be further divided into the following two groups [110].

##### 1. Stator armature

This improvement category includes items 1-4 in Table

2.

- *Auxiliary teeth and slots.* If the permanent magnet motor matches a suitable slot-pole combination, the low-order armature magnetic potential harmonics of the motor can be eliminated or at least reduced [111].
- *Slot bridge of stator.* The presence of cogging torque is mainly caused by the slotting in the stator. Making a bridge connection between the adjacent tooth can help minimizing cogging torque [112].
- *Slot width.* The cogging torque can be calculated according to the following equation [113]:

$$\begin{cases} T_c = \left( \frac{dW_a}{d\theta} \right)_{i=\text{const.}} \\ W_a = \frac{1}{2\mu_0} \int_v B^2 dV \end{cases} \quad (2)$$

Here  $W_a$  is the co-energy,  $B$  is the flux density, and  $\mu_0$  is the vacuum permeability. Furthermore, it can be seen from Eqs. (1)- (2) that the larger the

slot width is, the greater is the cogging torque. Therefore, if a reduction of the cogging torque is desired, the width of the slot should be reduced as much as possible [114].

- *Air-Gap Profile.* The cogging torque decreases with increased air-gap length [115], the proper increment of air-gap length can significantly weaken the cogging torque [116]. By choosing the correct dip and dip angle, the amplitude of higher order harmonics of the cogging torque can be reduced substantially [117].

##### 2. Magnetic pole

This part includes items 5-8 in Table 2.

- *Magnet pole arc.* The magnetic poles are designed to be positioned at a certain angle, with the aim to reduce the focused magnetic flux between the two poles. Adjusting the angle stabilizes the electromagnetic force of the magnetic pole acting on the stator teeth, and a smaller cogging torque is generated in the machine [122].
- *PM Surface Shape.* The magnet shape determines the distribution of the magnetic field in the air-gap, while the optimization of the magnetic-pole shape enhances  $B_t$  and  $B_n$  and reduces torque ripple [130].
- *Skewing of the PM.* The cogging torque is the sum of a series of cogging torque harmonics. The correct skew mode can be helpful in canceling the magnets' harmonics cogging-torque [131].
- *Segmenting of PM.* The radially magnetized arc of the magnetic pole is divided into several radially magnetized arc blocks, which can significantly reduce the cogging torque. By placing each magnetic block suitably, the low-order harmonics of the cogging torque can be reduced or even fully eliminated [128].

In SRMs and IMs, both stator and rotor consist of armature windings, and the items 1-4 in Table 2 can be similarly used as a reference [70]. These methods include the use of auxiliary teethtes/slots, and an improved air-gap profile among other options [132]. A comparison for vibration optimizations of different types of motors is shown in Table 3.

##### B. Controller Design

The optimization of the motor structure and configuration can only reduce vibration in electric motors, but not eliminate it completely [133]. Moreover, unusual designs may increase the complexity of the production process, which increases cost. Another approach is to improve the voltage and current control methods, which allows to correct the nonideal characteristics of the machine actively [82]. Electric motors have several control modes, with a wide range of varying stator armature currents. This means there are substantial differences in the armature EMF with respect to its interaction when considering the rotor EMF [134]. Table 4 summarizes the control methods to reduce vibration in IWMs that can be found in the literature.

The control methods can be summarized as follows:

Table 2 Optimization of the PMSM/BLDC structure.

According to the internal causes of motor vibration, the structure optimization is mainly focused on stator teeth and rotor PMs.

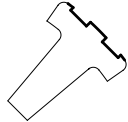

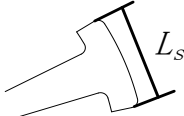
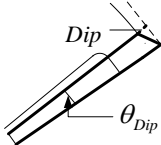
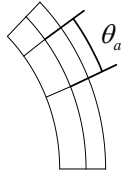
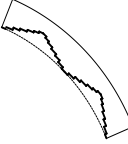
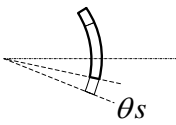
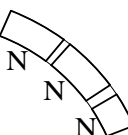
No.	Figure	Optimization	Purpose	Structure Parameters	Results
Changed parameters of the stator armature					
1.		Auxiliary teethest/slots	Cogging torque (peak to peak)	8-poles 6-slots	12.74→1.96 Nm [111]
				4-poles 12slots	1.25→0.25 Nm [116]
2.		Slot bridge of stator	Torque ripple (peak to peak)	10-poles 12-slots	0.40→0.13 Nm [118]
3.		Slot width - $L_s$	Cogging torque (peak to peak)	10-poles 12-slots	0.064.8→0.039.8 Nm [119]
4.		Air-Gap Profile- $\theta_{Dip}$	Amplitude of harmonics of cogging torque	6-poles 6-slots	0.0045→0.0005 Nm (3 <sup>th</sup> harmonic) [117]
				4-poles 4-slots	0.0097→0.00154 Nm (1 <sup>th</sup> harmonic) [120]
				8-poles 8-slots	70→35 $\mu$ Nm (1 <sup>th</sup> harmonic) [115]
				Changing design parameters of the magnetic pole	
5.		Magnet pole arc- $\theta_a$	Torque ripple	24-poles 72-slots	30.57→2.49 % [121]
				6-poles 36-slots	17.26→2.73 % [121]
				8-poles 12-slots	35.11→5.64% [122]
6.		PM Surface Shape	Cogging torque (peak to peak)	4-poles 12-slots	1.770→0.716 Nm [123]
				28-poles 5-slots	0.055→0.001 Nm [124]
7.		Skewing of the PM- $\theta_s$	Cogging torque (peak to peak)	6-poles 17-slots	17→3 Nm [125]
				4-poles 6-slots	0.025→0.0072 Nm [126]
				8-poles 48-slots	3.72→2.98 Nm [127]
8.		Segmenting of PM	Cogging torque (peak to peak)	4-poles 24-slots	225→50 Nm [128]
				9-poles 36-slots	3.22→0.089 Nm [129]

Table 3 Comparison of four types of motors.

	SRM	IM
<b>Similar approach to PMSM/BLDC</b>	<ul style="list-style-type: none"> <li>● Skewing stator and rotor [135];</li> <li>● Modifying stage arc angles [136];</li> <li>● Adjusting the shape of the stator [137];</li> <li>● Segmenting of armature winding [97].</li> </ul>	
<b>Unique approach</b>	<ul style="list-style-type: none"> <li>● Optimizing the angle of the double salient structure [138].</li> </ul>	<ul style="list-style-type: none"> <li>● Using asymmetrical straight rotor bars [139].</li> </ul>

Table 4 Classification of the vibration control methods.

Method	Method Strategy	Motor	Purpose and Result
<b>(a) Active vibration cancellation (AVC)</b>			
AVC	A two-step voltage control method with constant-period zero-voltage excitation.	SRM 4-kW	Vibration due to voltage variation at turn-off is reduced by 50% [140]
AVC by Pulse-Width Modulation (PWM)	Each single PWM channel is used to generate each single gate signal.	SRM 230-W	Vibration caused by PWM harmonics is reduced by 10% [141]
Magnetic excitation	Two individual three-phase winding PWM carriers.	PMSM 70-kW (Max)	Vibration due to the carrier harmonic component is reduced by a 50% [64]
<b>(b) Control of current chopping (CCC)</b>			
CCC	The feedback signal of the vibration acceleration response determines the phase current.	SRM 5-kW	Unbalanced radial force is reduced by 27.3% [26, 142]
Independent phase of CCC	The feedback signal becomes the vibration acceleration for each phase.	SRM 3-kW	Unbalanced radial force is reduced by 78.9% [102]
CCC based on $d-q$ reference frame	The optimized phase current waveform is based on the $d-q-0$ reference frame.	BLDC 400-W	Torque ripple exhibits no pulsation [85]
<b>(c) Methods of direct control</b>			
Feedback linearization direct torque control	Feedback linearization of the nonlinear motor model is carried out to obtain the equivalent linearization model.	PMSM 390-W	Torque and flux ripples reduced by 4.6% and 6.8% [143]
Direct instantaneous force control	Adjusting the switch angle to limit the current-change rate and control of the overall radial force.	SRM 46.5-kW	Smooth overall radial force [144]
<b>(d) Defining the phase current command</b>			
Current regulation by fuzzy logic	Fuzzy logic is used to inject a compensation current into each phase.	SRM 1.5-kW	Radial force is reduced by 30.4%. Torque ripple is reduced by 33% [145].
Harmonic injection method	Adding a harmonic current to the excitation current to counteract vibration.	PMSM 750-W	The maximal peak-to-peak torque pulsation is reduced to 33.3% [146]
Third harmonic current injection	A third-order harmonic current is injected into the motor.	PMSM 100-kW	The ratio of peak-to-peak torque ripple to average torque is reduced from 7.6% to 3.6% [147]
Defining current profile method	Defining the current properly reference of the injected motor.	SRM 1-kW	The sum of the radial force is reduced to 45.66% [148].
		785-W 393-W	The third-order harmonic component is reduced by 93% [149, 150]

- *Active vibration cancellation:* This method focuses on the vibration induced by voltage variation in the turn-off phase. It introduces a two-step voltage waveform with a constant period of zero-voltage excitation [140]. Subsequently, the PWM and magnetic excitation technique are incorporated in the AVC, which can suppress harmonics accurately [141].
- *Control of current chopping:* This method focuses on the vibration caused by an unbalanced radial

force. The acceleration feedback signal is selected to determine the chopping-current threshold and PWM duty cycle [26]. The UEMF can be reduced using the independent chopping method for each channel [102]. In addition, based on the  $d-q$  reference frame, the torque ripple can be eliminated [85].

- *Direct control:* Conventional direct control has some drawbacks such as large torque ripple and a fast-changing switching frequency [151]. The

improvements in the novel direct control algorithms include: 1) Decoupling and linearization from the nonlinear coupling model, and usage of the more mature linear control theory to reduce flux pulsation [143]. 2) Keeping the overall radial force unchanged during the direct control of the electromagnetic force [144].

- *Direct phase current control:* This method focuses on the optimization of the excitation current. While this approach uses a wide range of correction- or injection-current methods, two types can be distinguished: 1) Decreasing both the maximum radial force and the maximal peak-to-peak torque pulsation by injecting a compensation current into each phase, which also minimizes them [145]. 2) A higher order harmonic current is added [146]. The third-harmonic current injection method [147], especially, allows the radial forces to add up to a constant sum, which reduces the harmonics of the radial force [148].

### C. Additional control components

Another way to reduce vibration is to regard the IWM-suspension as a whole system and perform a well-developed suspension optimization and control algorithm. Similar to conventional suspension system designs, the parameter optimization for the passive system is described in [152], where the parameters of the wheel spring and rubber sleeve are optimized. If the electromagnetic dynamics are ignored, the IWM can be regarded as an additional mass that is added to the unsprung mass. Many studies focused on using conventional suspension-control algorithms to reduce the negative impact of the increased unsprung mass. Examples for these algorithms include PID [153], ceiling damping control [154], optimal sliding mode [155], linear parameter variation, frequency estimation-based [156], constrained adaptive back-stepping multi-objective control [157], and generalized predictive control [158].

Another approach is to design a novel dynamic vibration absorbing structure (DVAS), which is situated between the IWM and the suspension to absorb the IWM vibration. The new structure does not change the original structure of the vehicle suspension [23]. The DVAS structure can be seen in Fig. 10.

The DVAS consists of a spring and an internal damper, and the DVAS damper can be continuously adjusted to reduce the motor stator vibration and isolate the force transmitted to the motor bearing [29]. Compared with the conventional IWM structure, DVAS can effectively improve ride comfort and reduce IWM vibration [27, 30].

## V. OUTLOOK

The previous sections represent comprehensive state-of-the-art reviews that include modeling, vibration-source analysis, and vibration reduction techniques for IWMs. In this section, an outlook for vibration improvements in IWM-driven EVs is provided.

### A. Future trends for improvements of internally-induced motor vibration

1. *Modelling accuracy.* Additional vibration mitigation requires a more accurate vibration analysis model for system dynamics, loss calculations, demagnetization analysis, and thermal characteristics. An accurate model should also describe both the radial force and the tangential force of the motor precisely. In addition, a more accurate lifespan model should be developed to better understand the relationship between motor vibration and the lifespan of EVs.

2. *Vibration-mitigation methods.* Using a more accurate system model, more effective control methods and better optimized motor structures as well as more efficient cooling methods should be developed to suppress vibration of IWMs. And the particularly important is the elimination of magnetic field harmonics.

### B. Future trends for coupling effects of IWM-suspension

Future studies of IWM-suspensions could focus on a deeper understanding of coupling effects, especially for complex operating conditions.

1. *In-depth study of coupling effects.* The effect of the IWM vibrations on the vehicle's stability and ride comfort should be studied in more detail. Specifically, more investigations should be made to better understand the vertical, lateral, and longitudinal coupling dynamics for different driving conditions, including different *RG* and *RT* - especially when low torque is produced for creeping and high torque for climbing.

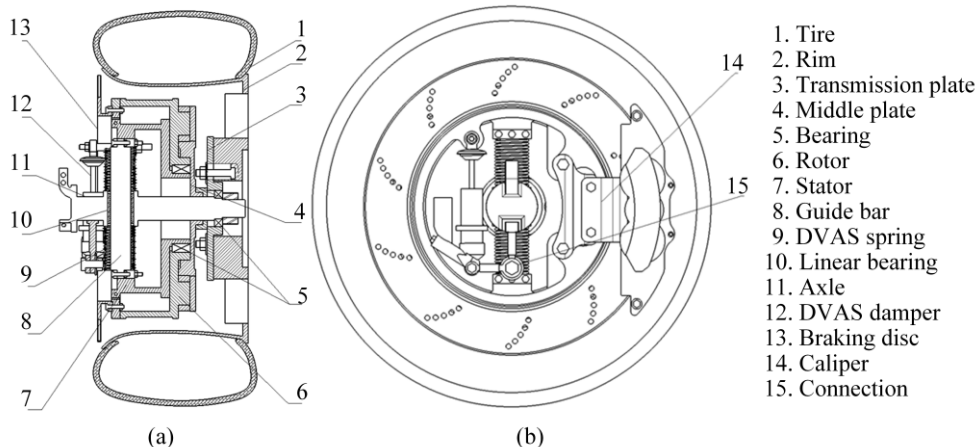


Fig. 10. Structure of the DVAS based IWM-suspension system: (a) side view (b) front view. [23]

2. *Coupling effects with chassis control modules.* Apart from studying the coupling effect in terms of dynamics, coupling between IWMs and other chassis control modules should also be investigated in more detail. Furthermore, the interaction between IWMs and traction control systems, anti-lock brake systems, and electronic stability-control systems should be clarified, by considering the four-quadrant operation of the motor (forward braking, forward motoring, reverse motoring and reverse braking). All interdependent parameters for electro-mechanical coupling are needed to be taken into account.

### C. Future trends for the vibration reduction of IWMs

Future vibration mitigation measures of IWMs will likely focus on the integrated design and optimization of the IWM-suspension.

1. *Control strategy.* Reducing the vibration caused by coupling effects of the IWM-suspension system should be possible by improving the control algorithm. There are negative interaction effects between vehicle suspension and the IWM's absorber. A study to develop more advanced control methods for the IWM system to overcome these effects would be highly desired.

2. *Optimization of the DVAS.* The vibration can also be reduced by improving the DVAS performance. In particular, the role and effect of stability and ride comfort, e.g. damping and stiffness of the isolator, can benefit from further studies.

3. *Experimental validation.* More tests using specialized test platforms and real systems should be performed to verify the effectiveness of different control methods.

## VI. CONCLUSION

This review summarized the vibration sources and mitigation methods for IWM-driven EVs. The motor-selection criteria were described, followed by a brief introduction and a multidimensional comparison of different motor types. Subsequently, both torque and radial force mechanics were discussed, different motor-modeling processes were described, and electro-mechanical-magnetic coupling effects were summarized. Both internal and external vibration-sources were reviewed, and the longitudinal-vertical IWM-suspension coupling effect was presented. Furthermore, methods to optimize the motor structure were discussed. Motor controller, traditional suspension-control methods, and additional control components to improve the NVH performance were summarized and compared. Several promising improvement strategies of the motor dynamics and IWM-driven EVs were described at the end. The review represents a compact overview of the latest developments and trends regarding vibrations in IWM-driven EVs, which is designed to aid researchers (both experienced and newcomers to the field) to conduct a multidisciplinary analysis and find important optimization criteria in the rapidly developing field of IWM vibration control.

## REFERENCES

- [1] B. Li, H. Du, W. Li, et al., "Dynamically integrated spatiotemporal-based trajectory planning and control for autonomous vehicles," *IET Intell. Transp. Sys.*, vol. 12, pp. 1271-1282, 2018.
- [2] B. Li, H. Du, W. Li, "A potential field approach-based trajectory control for autonomous electric vehicles with in-wheel motors," *IEEE Trans. Intell. Transp.*, vol. 18, pp. 2044-2055, 2016.
- [3] H. Taghavifar, C. Hu, Y. Qin, et al., "EKF-Neural Network Observer Based Type-2 Fuzzy Control of Autonomous Vehicles," *IEEE Trans. Intell. Transp.*, vol. 99, pp. 1-13, 2020.
- [4] C. Hu, H. Gao, J. Guo, et al., "RISE-Based Integrated Motion Control of Autonomous Ground Vehicles With Asymptotic Prescribed Performance," *IEEE Trans. Syst. Man. Cy-S.*, vol. 99, 2019.
- [5] Chuan Hu, Hongbo Gao, Jinghua Guo, Hamid Taghaviar, Yechen Qin, Jing Na, Chongfeng Wei, "RISE-Based Integrated Motion Control of Autonomous Ground Vehicles with Asymptotic Prescribed Performance," *IEEE Trans. Syst. Man. Cy-S.*, 2019.
- [6] Chuan Hu, Zhenfeng Wang, Hamid Taghavifar, Jing Na, Yechen Qin, Jinghua Guo, Chongfeng Wei, "MME-EKF-Based Path-Tracking Control of Autonomous Vehicles Considering Input Saturation," *IEEE Trans. Veh. Technol.*, vol. 68, pp. 52, 2019.
- [7] S. Zuo, F. Lin, X. Wu, et al., "Calculation, and Reduction of External Rotor Permanent-Magnet Synchronous Motor," *IEEE Trans. Ind. Electron.*, vol. 62, pp. 6204-6212, 2015.
- [8] J. Ni, J. Hu, C. Xiang, "Envelope control for four-wheel independently actuated autonomous ground vehicle through AFS/DYC integrated control," *IEEE Trans. Veh. Technol.*, vol. 66, pp. 9712-9726, 2017.
- [9] J. Ni, J. Hu, C. Xiang, "A review for design and dynamics control of unmanned ground vehicle," *P. I. Mech. Eng. D-J. Aut.*, vol. 235, no. 4, 2020. 0954407020 912097.
- [10] Y. Qin, E. Hashemi, A. Khajepour, "Integrated Crash Avoidance and Mitigation Algorithm for Autonomous Vehicles," *IEEE Trans. Ind. Inform.*, 2021.
- [11] S. Derammelaere, M. Haemers, J. De Viaene, et al., "A quantitative comparison between BLDC, PMSM, Brushed DC and Stepping Motor Technologies," *ICEMS.*, pp. 1-5, 2016.
- [12] K. Bienkowski, J. Szczypior, B. Bucki, et al., "A. Rogalski, Influence of geometrical parameters of Switched Reluctance Motor on electromagnetic torque," *P. XVI. ICEMK.*, pp. 5-8, 2004.
- [13] W. Zhu, B. Fahimi, S. Pekarek, "A Field Reconstruction Method for Optimal Excitation of Permanent Magnet Synchronous Machines," *IEEE Trans. Energy. Convers.*, vol. 21, pp. 305-313, 2006.
- [14] Weida Wang, Kaijia Liu, Chao Yang, Bin Xu, and Mingyue Ma. "Cyber physical energy optimization control design for PHEVs based on enhanced firework algorithm," *IEEE Trans. Veh. Technol.*, vol. 70, iss. 1, pp.282-291, 2021.
- [15] R. Islam, I. Husain, "Analytical model for predicting noise and vibration in permanent-magnet synchronous motors," *IEEE Trans. Ind. Appl.*, vol. 46, pp. 2346-2354, 2010.
- [16] Z.Q. Zhu, D. Ishak, D. Howe, J. Chen, "Unbalanced Magnetic Forces in Permanent-Magnet Brushless Machines With Diametrically Asymmetric Phase Windings," *IEEE*

*Trans. Ind. Appl.*, vol. 43, pp. 1544-1553, 2007.

- [17] D.G. Dorrell, "Calculation of unbalanced magnetic pull in cage induction machines," *University of Cambridge*, 1993.
- [18] U. Kim, D.K. Lieu, "Effects of magnetically induced vibration force in brushless permanent-magnet motors," *IEEE Trans. Magn.*, vol. 41, pp. 2164-2172, 2005.
- [19] S.H. Kia, H. Henao, G. Capolino, "Torsional Vibration Assessment Using Induction Machine Electromagnetic Torque Estimation," *IEEE Trans. Ind. Electron.*, vol. 57, pp. 209-219, 2010.
- [20] K. Vijayakumar, R. Karthikeyan, S. Paramasivam, et al., "Switched Reluctance Motor Modeling, Design, Simulation, and Analysis: A Comprehensive Review," *IEEE Trans. Magn.*, vol. 44, pp. 4605-4617, 2008.
- [21] Y. Qin, J.J. Rath, C. Hu, et al., "Adaptive nonlinear active suspension control based on a robust road classifier with a modified super-twisting algorithm," *Nonlinear Dynamics*, vol. 97, pp. 2425-2442, 2019.
- [22] Y. Qin, Z. Wang, C. Xiang, E. Hashemi, A. Khajepour, Y. Huang, "Speed independent road classification strategy based on vehicle response: Theory and experimental validation," *Mech. Syst. Signal. Pr.*, vol. 117, pp. 653-666, 2019.
- [23] Y. Qin, C. He, X. Shao, H. Du, C. Xiang, M. Dong, "Vibration mitigation for in-wheel switched reluctance motor driven electric vehicle with dynamic vibration absorbing structures," *J. Sound. Vib.*, vol. 419, pp. 249-267, 2018.
- [24] X. Shao, F. Naghdy, H. Du, Y. Qin, "Coupling effect between road excitation and an in-wheel switched reluctance motor on vehicle ride comfort and active suspension control," *J. Sound. Vib.*, vol. 443, pp. 683-702, 2019.
- [25] J. Svendenius, M. Gäfvert, "A semi-empirical dynamic tire model for combined-slip forces," *Vehicle. Syst. Dyn.*, vol. 44, pp. 189-208, 2006.
- [26] W. Sun, Y. Li, J. Huang, N. Zhang, "Vibration effect and control of In-Wheel Switched Reluctance Motor for electric vehicle," *J. Sound. Vib.*, vol. 338, pp. 105-120, 2015.
- [27] B. Xu, C. Xiang, Y. Qin, P. Ding, M. Dong, "Semi-active vibration control for in-wheel switched reluctance motor driven electric vehicle with dynamic vibration absorbing structures: Concept and validation," *IEEE Access*, vol. 6, pp. 60274-60285, 2018.
- [28] M.S. Carmeli, F.C. Dezza, M. Mauri, "Electromagnetic vibration and noise analysis of an external rotor permanent magnet motor," *SPEEDAM*, pp. 1028-1033, 2006.
- [29] Weida Wang, Tianqi Qie, and Chao Yang, "An Intelligent Lane-Changing Behavior Prediction and Decision-Making Strategy for an Autonomous Vehicle," *IEEE Trans. Ind. Electron.*, 2021.
- [30] Y. Qin, Z. Wang, K. Yuan, Y. Zhang, "Comprehensive Analysis and Optimization of Dynamic Vibration-Absorbing Structures for Electric Vehicles Driven by In-Wheel Motors," *Automotive Innovation*, vol. 2, pp. 254-262, 2019.
- [31] Y. Qin, X. Tang, T. Jia, Z. Duan, J. Zhang, Y. Li, L. Zheng, "Noise and vibration suppression in hybrid electric vehicles: State of the art and challenges," *Renew. Sust. Energ. Rev.*, vol. 124, pp. 109782, 2020.
- [32] M. Valavi, A. Nysveen, R. Nilssen, "Magnetic forces and vibration in permanent magnet machines with non-overlapping concentrated windings: A review," *IEEE ICIT*, pp. 977-984, 2012.
- [33] S. Murata, "Innovation by in-wheel-motor drive unit," *Vehicle. Syst. Dyn.*, vol. 50, pp. 807-830, 2012.
- [34] L. Kumar, S. Jain, "Electric propulsion system for electric vehicular technology: A review," *Renew. Sust. Energ. Rev.*, vol. 29, pp. 924-940, 2014.
- [35] C. Bianchini, F. Immovilli, E. Lorenzani, A. Bellini, M. Davoli, "Review of design solutions for internal permanent-magnet machines cogging torque reduction," *IEEE Trans. Magn.*, vol. 48, pp. 2685-2693, 2012.
- [36] J. Wang, X. Yuan, K. Atallah, "Design optimization of a surface-mounted permanent-magnet motor with concentrated windings for electric vehicle applications," *IEEE Trans. Veh. Technol.*, vol. 62, pp. 1053-1064, 2012.
- [37] X. Xue, K.W.E. Cheng, T.W. Ng, N.C. Cheung, "Multi-objective optimization design of in-wheel switched reluctance motors in electric vehicles," *IEEE Trans. Ind. Electron.*, vol. 57, pp. 2980-2987, 2010.
- [38] M.-T. Peng, T.J. Flack, "Design and Analysis of an In-Wheel Motor With Hybrid Pole-Slot Combinations," *IEEE Trans. Magn.*, vol. 52, pp. 1-8, 2016.
- [39] J.-R. Riba, C. López-Torres, L. Romeral, A. Garcia, "Rare-earth-free propulsion motors for electric vehicles: A technology review," *Renew. Sust. Energ. Rev.*, vol. 57, pp. 367-379, 2016.
- [40] J.F. Gieras, "Advancements in electric machines," *Springer Science & Business Media*, 2008.
- [41] T. Sutikno, N.R.N. Idris, A. Jidin, "A review of direct torque control of induction motors for sustainable reliability and energy efficient drives," *Renew. Sust. Energ. Rev.*, vol. 32, pp. 548-558, 2014.
- [42] S.K. Panda, J.-X. Xu, W. Qian, "Review of torque ripple minimization in PM synchronous motor drives," *IEEE PES-CDEE*, pp. 1-6, 2008.
- [43] X. Gao, X. Wang, Z. Li, Y. Zhou, "A review of torque ripple control strategies of switched reluctance motor," *IJCAS*, vol. 8, pp. 103-116, 2015.
- [44] I. Boldea, L.N. Tutelea, L. Parsa, D. Dorrell, "Automotive electric propulsion systems with reduced or no permanent magnets: An overview," *IEEE Trans. Ind. Electron.*, vol. 61, pp. 5696-5711, 2014.
- [45] J. Faiz, E. Mazaheri-Tehrani, "Demagnetization modeling and fault diagnosing techniques in permanent magnet machines under stationary and nonstationary conditions: An overview," *IEEE Trans. Ind. Appl.*, vol. 53, pp. 2772-2785, 2016.
- [46] Y. Gessese, A. Binder, B. Funieru, "Analysis of the effect of radial rotor surface grooves on rotor losses of high speed solid rotor induction motor," *SPEEDAM 2010*, pp. 1762-1767, 2010.
- [47] W. Fei, P. Luk, K. Jinupun, "A new axial flux permanent magnet Segmented-Armature-Torus machine for in-wheel direct drive applications," *IEEE PESC*, pp. 2197-2202, 2008.
- [48] X. Xue, K. Cheng, N. Cheung, "Selection of electric motor drives for electric vehicles," *AUPEC*, pp. 1-6, 2008.
- [49] M. Zeraoulia, M.E.H. Benbouzid, D. Diallo, "Electric

- Motor Drive Selection Issues for HEV Propulsion Systems: A Comparative Study," *IEEE Trans. Veh. Technol.*, vol. 55, pp. 1756-1764, 2006.
- [50] S. Sakunthala, R. Kiranmayi, P.N. Mandadi, "A study on industrial motor drives: Comparison and applications of PMSM and BLDC motor drives," *ICECDS*, pp. 537-540, 2017.
- [51] E. Machacek, N. Fold, "Alternative value chains for rare earths: The Anglo-deposit developers," *Resources Policy*, vol. 42, pp. 53-64, 2014.
- [52] G. Wu, X. Zhang, Z. Dong, "Powertrain architectures of electrified vehicles: Review, classification and comparison," *J. Franklin. I.*, vol. 352, pp. 425-448, 2015.
- [53] D.G. Dorrell, A.M. Knight, M. Popescu, L. Evans, D.A. Staton, "Comparison of different motor design drives for hybrid electric vehicles," *IEEE ECCE*, pp. 3352-3359, 2010.
- [54] A. Chiba, M. Takeno, N. Hoshi, M. Takemoto, S. Ogasawara, M.A. Rahman, "Consideration of Number of Series Turns in Switched-Reluctance Traction Motor Competitive to HEV IPMSM," *IEEE Trans. Ind. Appl.*, vol. 48, pp. 2333-2340, 2012.
- [55] A. Chiba, K. Kiyota, N. Hoshi, M. Takemoto, S. Ogasawara, "Development of a Rare-Earth-Free SR Motor With High Torque Density for Hybrid Vehicles," *IEEE Trans. Energy. Conver.*, vol. 30, pp. 175-182 2015.
- [56] W. Deng, S. Zuo, "Analytical Modeling of the Electromagnetic Vibration and Noise for an External-Rotor Axial-Flux in-Wheel Motor," *IEEE Trans. Ind. Electron.*, vol. 65, pp. 1991-2000, 2018.
- [57] Y. Luo, D. Tan, "Research on the Hub-motor Driven Wheel Structure with a Novel Built-in Mounting System," *Automotive Engineering*, vol. 35, pp. 1105-1110, 2013.
- [58] Y. Fang, T. Zhang, "Vibroacoustic characterization of a permanent magnet synchronous motor powertrain for electric vehicles," *IEEE Trans. Energy. Conver.*, vol. 33, pp. 272-280, 2017.
- [59] Y. Yu, L. Zhao, C. Zhou, "Influence of rotor-bearing coupling vibration on dynamic behavior of electric vehicle driven by in-wheel motor," *IEEE Access*, vol. 7, pp. 63540-63549, 2019.
- [60] M. Anwar, O. Husain, "Radial force calculation and acoustic noise prediction in switched reluctance machines," *IEEE Trans. Ind. Appl.*, vol. 36, pp. 1589-1597, 2000.
- [61] E. Devillers, M. Hecquet, J. Le Besnerais, "Effect of tangential flux density on radial magnetic force for the vibroacoustic study of induction machines at no-load and load state." 2016.
- [62] W. Deng, S. Zuo, "Electromagnetic vibration and noise of the permanent-magnet synchronous motors for electric vehicles: An overview," *IEEE Trans. Transp. Electr.*, vol. 5, pp. 59-70, 2018.
- [63] J. Le Besnerais, "Fast prediction of variable-speed acoustic noise due to magnetic forces in electrical machines," *ICEM*, pp. 2259-2265, 2016.
- [64] Y. Miyama, M. Ishizuka, H. Kometani, K. Akatsu, "Vibration Reduction by Applying Carrier Phase-Shift PWM on Dual Three-Phase Winding Permanent Magnet Synchronous Motor," *IEEE Trans. Ind. Appl.*, vol. 54, pp. 5998-6004, 2018.
- [65] W. Zhu, S. Pekarek, B. Fahimi, B.J. Deken, "Investigation of Force Generation in a Permanent Magnet Synchronous Machine," *IEEE Trans. Energy. Conver.*, vol. 22, pp. 557-565, 2007.
- [66] J. Pyrhonen, T. Jokinen, V. Hrabovcova, "Design of rotating electrical machines," *JW. A.*, 2013.
- [67] F. Lin, S. Zuo, X. Wu, "Electromagnetic vibration and noise analysis of permanent magnet synchronous motor with different slot-pole combinations," *IET. Electr. Power. App.*, vol. 10, pp. 900-908, 2016.
- [68] J. Hallal, A.H. Rasid, F. Druessne, V. Lanfranchi, "Comparison of radial and tangential forces effect on the radial vibrations of synchronous machines," *IEEE ICIT*, pp. 243-248, 2019.
- [69] J.F. Gieras, C. Wang, J.C. Lai, "Noise of polyphase electric motors," *CRC press*, 2018.
- [70] T. Ito, K. Akatsu, "Electromagnetic force acquisition distributed in electric motor to reduce vibration," *IEEE Trans. Ind. Appl.*, vol. 53, pp. 1001-1008, 2016.
- [71] S. Wang, J. Hong, Y. Sun, J. Shen, H. Cao, Z. Yang, "Analysis and experimental verification of electromagnetic vibration mode of PM brush DC motors," *IEEE Trans. Energy. Conver.*, vol. 33, pp. 1411-1421, 2018.
- [72] H. Guldemir, "Detection of airgap eccentricity using line current spectrum of induction motors," *Electr. Pow. Syst. Res.*, vol. 64, pp. 109-117, 2003.
- [73] S. Nandi, S. Ahmed, H.A. Toliyat, "Detection of rotor slot and other eccentricity related harmonics in a three phase induction motor with different rotor cages," *IEEE Trans. Energy. Conver.*, vol. 16, pp. 253-260, 2001.
- [74] C. Bi, Q. Jiang, S. Lin, T.S. Low, A.A. Mamun, "Reduction of acoustic noise in FDB spindle motors by using drive technology," *IEEE Trans. Magn.*, vol. 39, pp. 800-805, 2003.
- [75] F. Liu, C. Xiang, H. Liu, L. Han, Y. Wu, X. Wang, P. Gao, "Asymmetric effect of static radial eccentricity on the vibration characteristics of the rotor system of permanent magnet synchronous motors in electric vehicles," *Nonlinear Dynamics*, vol. 96, pp. 2581-2600 2019.
- [76] A. Smith, D. Dorrell, "Calculation and measurement of unbalanced magnetic pull in cage induction motors with eccentric rotors. Part 1: Analytical model," *IEE. P-ELECT. Pow. Appl.*, vol. 143, pp. 193-201, 1996.
- [77] T.-J. Kim, S.-M. Hwang, N.-G. Park, "Analysis of vibration for permanent magnet motors considering mechanical and magnetic coupling effects," *IEEE Trans. Magn.*, vol. 36, pp. 1346-1350, 2000.
- [78] P. Vijayraghavan, R. Krishnan, "Noise in electric machines: A review," *IEEE Trans. Ind. Appl.*, vol. 35, pp. 1007-1013, 1999.
- [79] D.E. Cameron, J.H. Lang, S.D. Umans, "The origin and reduction of acoustic noise in doubly salient variable-reluctance motors," *IEEE Trans. Ind. Appl.*, vol. 28, pp. 1250-1255, 1992.
- [80] J. Krotsch, B. Piepenbreier, "Radial Forces in External Rotor Permanent Magnet Synchronous Motors With Non-Overlapping Windings," *IEEE Trans. Ind. Electron.*, vol. 59, pp. 2267-2276, 2012.

- [81] T. Miller, M. Popescu, C. Cossar, M. McGilp, "Computation of the voltage-driven flux-MMF diagram for saturated PM brushless motors," *IAS.*, pp. 1023-1028, 2005.
- [82] D.C. Hanselman, "Minimum torque ripple, maximum efficiency excitation of brushless permanent magnet motors," *IEEE Trans. Ind. Electron.*, vol. 41, pp. 292-300, 1994.
- [83] Z.Q. Zhu, J.H. Leong, "Analysis and Mitigation of Torsional Vibration of PM Brushless AC/DC Drives With Direct Torque Controller," *IEEE Trans. Ind. Appl.*, vol.48, pp. 1296-1306, 2012.
- [84] Z. Liu, J. Li, "Accurate prediction of magnetic field and magnetic forces in permanent magnet motors using an analytical solution," *IEEE Trans. Energy. Conver.*, vol. 23, pp. 717-726, 2008.
- [85] S.J. Park, H.W. Park, M.H. Lee, F. Harashima, "A new approach for minimum-torque-ripple maximum-efficiency control of BLDC motor," *IEEE Trans. Ind. Electron.*, vol. 47, pp. 109-114, 2000.
- [86] P. Donolo, G. Bossio, C. De Angelo, G. García, M. Donolo, "Voltage unbalance and harmonic distortion effects on induction motor power, torque and vibrations," *Electr. Pow. Syst. Res.*, vol. 140, pp. 866-873, 2016.
- [87] G. Narayanan, V. Ranganathan, "Analytical evaluation of harmonic distortion in PWM AC drives using the notion of stator flux ripple," *IEEE Trans. Power. Electr.*, vol. 20, pp. 466-474, 2005.
- [88] N.R.N. Idris, A.H.M. Yatim, "Direct Torque Control of Induction Machines With Constant Switching Frequency and Reduced Torque Ripple," *IEEE Trans. Ind. Electron.*, vol. 51, pp. 758-767, 2004.
- [89] A. Khalil, I. Husain, "A fourier series generalized geometry-based analytical model of switched reluctance machines," *IEEE Trans. Ind. Appl.*, vol. 43, pp. 673-684, 2007.
- [90] H. Li, B. Bilgin, A. Emadi, "Effects of Current Excitation on Nodal Forces in Switched Reluctance Motors," *IEEE ITEC.*, pp. 761-766, 2018.
- [91] K. Hameyer, R.J. Belmans, "Permanent magnet excited brushed DC motors," *IEEE Trans. Ind. Electron.*, vol. 43, pp. 247-255, 1996.
- [92] Y. Liu, Z.Q. Zhu, D. Howe, "Direct Torque Control of Brushless DC Drives With Reduced Torque Ripple," *IEEE Trans. Ind. Appl.*, vol. 41, pp. 599-608, 2005.
- [93] K.-T. Kim, K.-M. Hwang, G.-Y. Hwang, T.-J. Kim, W.-B. Jeong, C.-U. Kim, "Effect of rotor eccentricity on spindle vibration in magnetically symmetric and asymmetric BLDC motors," *IEEE ISIE.*, pp. 967-972, 2001.
- [94] A.K. Wallace, R. Spee, L.G. Martin, "Current harmonics and acoustic noise in AC adjustable-speed drives," *IEEE Trans. Ind. Appl.*, vol. 26, pp. 267-273, 1990.
- [95] A.A. Shaltout, "Analysis of torsional torques in starting of large squirrel cage induction motors," *IEEE Trans. Energy. Conver.*, vol. 9, pp. 135-142, 1994.
- [96] L.T.-P. Timár-P, P. Timár, "Noise and vibration of electrical machines," *North Holland*, 1989.
- [97] R. Madhavan, B.G. Fernandes, "Performance Improvement in the Axial Flux-Segmented Rotor-Switched Reluctance Motor," *IEEE Trans. Energy. Conver.*, vol. 29, pp. 641-651, 2014.
- [98] L. Ran, R. Yacamini, K. Smith, "Torsional vibrations in electrical induction motor drives during start-up," *J Vib Acoust.*, vol. 118, pp. 242-251, 1996.
- [99] A.K. Putri, S. Rick, D. Franck, K. Hameyer, "Application of sinusoidal field pole in a permanent-magnet synchronous machine to improve the NVH behavior considering the MTPA and MTPV operation area," *IEEE Trans. Ind. Appl.*, vol. 52, pp. 2280-2288, 2016.
- [100] Y. Mao, S. Zuo, X. Wu, X. Duan, "High frequency vibration characteristics of electric wheel system under in-wheel motor torque ripple," *J. Sound. Vib.*, vol. 400, pp. 442-456, 2017.
- [101] A. Arkkio, S. Cederström, H.A.A. Awan, S.E. Saarakkala, T.P. Holopainen, "Additional losses of electrical machines under torsional vibration," *IEEE Trans. Energy. Conver.*, vol. 33, pp. 245-251, 2017.
- [102] Z. Li, L. Zheng, W. Gao, Z. Zhan, "Electromechanical coupling mechanism and control strategy for in-wheel-motor-driven electric vehicles," *IEEE Trans. Ind. Electron.*, vol. 66, pp. 4524-4533, 2018.
- [103] Y. Qin, Z. Wang, C. Xiang, M. Dong, C. Hu, R. Wang, "A novel global sensitivity analysis on the observation accuracy of the coupled vehicle model," *Vehicle. Syst. Dyn.*, vol. 57, pp. 1445-1466, 2019.
- [104] Y. Luo, D. Tan, "Study on the dynamics of the in-wheel motor system," *IEEE Trans. Veh. Technol.*, vol. 61, pp. 3510-3518, 2012.
- [105] D. Tan, C. Lu, "The influence of the magnetic force generated by the in-wheel motor on the vertical and lateral coupling dynamics of electric vehicles," *IEEE Trans. Veh. Technol.*, vol. 65, pp. 4655-4668, 2015.
- [106] M. Biček, G. Gotovac, D. Miljavec, S. Zupan, "Mechanical failure mode causes of in-wheel motors," *Stroj. Vestn.-J. Mech. E.*, vol. 61, pp. 74-85, 2015.
- [107] G. Jang, D. Lieu, "The effect of magnet geometry on electric motor vibration," *IEEE Trans. Magn.*, vol. 27, pp. 5202-5204, 1991.
- [108] A. Pouramin, R. Dutta, M. Rahman, "Design optimization of a spoke-type FSCW IPM machine to achieve low torque ripple and high torque density under a wide constant power speed range," *2018 IEEE ECCE.*, pp. 6914-6921, 2018.
- [109] D. Wang, X. Wang, S.-Y. Jung, "Reduction on cogging torque in flux-switching permanent magnet machine by teeth notching schemes," *IEEE Trans. Magn.*, vol. 48, pp. 4228-4231, 2012.
- [110] D. Wang, X. Wang, M.-K. Kim, S.-Y. Jung, "Integrated Optimization of Two Design Techniques for Cogging Torque Reduction Combined With Analytical Method by a Simple Gradient Descent Method," *IEEE Trans. Magn.*, vol. 48, pp. 2265-2276, 2012.
- [111] C.S. Koh, J.-S. Seol, "New cogging-torque reduction method for brushless permanent-magnet motors," *IEEE Trans. Magn.*, vol. 39, pp. 3503-3506, 2003.
- [112] I. Hasan, Y. Sozer, A.P. Ortega, S. Paul, R. Islam, "Investigation of design based solutions to reduce vibration in permanent magnet synchronous machines with low order radial forces," *IEEE ECCE.*, pp. 5431-5437, 2017.

- [113] J.M. Ling, T. Nur, "Influence of edge slotting of magnet pole with fixed slot opening width on the cogging torque in inset permanent magnet synchronous machine," *Adv. Mech. Eng.*, vol. 8, no. 8, pp 1687814016659598, 2016.
- [114] S.-H. Lee, K.-K. Han, H.-J. Ahn, G.-H. Kang, Y.-D. Son, G.-T. Kim, "A study on reduction of vibration based on decreased cogging torque for interior type permanent magnet motor," *IEEE IAS*, pp. 1-6, 2008.
- [115] B.-I. Kwon, B.-Y. Yang, S.-C. Park, Y.-S. Jin, "Novel topology of unequal air gap in a single-phase brushless DC motor," *IEEE Trans. Magn.*, vol. 37, pp. 3723-3726, 2001.
- [116] C. Breton, J. Bartolome, J. Benito, G. Tassinario, I. Flotats, C. Lu, B. Chalmers, "Influence of machine symmetry on reduction of cogging torque in permanent-magnet brushless motors," *IEEE Trans. Magn.*, vol. 36, pp. 3819-3823, 2000.
- [117] M. Fazil, K.R. Rajagopal, "A Novel Air-Gap Profile of Single-Phase Permanent-Magnet Brushless DC Motor for Starting Torque Improvement and Cogging Torque Reduction," *IEEE Trans. Magn.*, vol. 46, pp. 3928-3932, 2010.
- [118] S. Das, I. Hasan, Y. Sozer, R. Islam, A.P. Ortega, J. Klass, "Noise and vibration performance in fractional slot permanent magnet synchronous machines using stator bridge," *IEEE ITEC*, pp. 632-637, 2018.
- [119] Y.-U. Park, J.-H. Cho, D.-k. Kim, "Cogging Torque Reduction of Single-Phase Brushless DC Motor With a Tapered Air-Gap Using Optimizing Notch Size and Position," *IEEE Trans. Ind. Appl.*, vol. 51, pp. 4455-4463, 2015.
- [120] C. Chun-Lung, C. Yie-Tone, J. Wun-Siang, "Properties of Cogging Torque, Starting Torque, and Electrical Circuits for the Single-Phase Brushless DC Motor," *IEEE Trans. Magn.*, vol. 44, pp 2317-2323, 2008.
- [121] D. Wang, X. Wang, S.-Y. Jung, "Cogging Torque Minimization and Torque Ripple Suppression in Surface-Mounted Permanent Magnet Synchronous Machines Using Different Magnet Widths," *IEEE Trans. Magn.*, vol. 49, pp. 2295-2298, 2013.
- [122] P. Ling, D. Ishak, T. Tiang, "Influence of magnet pole arc variation on the performance of external rotor permanent magnet synchronous machine based on finite element analysis," *IEEE PECon*, pp. 552-557, 2016.
- [123] N. Chen, S.L. Ho, W.N. Fu, "Optimization of Permanent Magnet Surface Shapes of Electric Motors for Minimization of Cogging Torque Using FEM," *IEEE Trans. Magn.*, vol. 46, pp. 2478-2481, 2010.
- [124] F. Scuiller, "Magnet Shape Optimization to Reduce Pulsating Torque for a Five-Phase Permanent-Magnet Low-Speed Machine," *IEEE Trans. Magn.*, vol. 50, pp. 1-9, 2014.
- [125] T. Liu, S. Huang, J. Gao, "A method for reducing cogging torque by magnet shifting in permanent magnet machines," *ICEMS*, pp. 1073-1076, 2010.
- [126] Z. Wenliang, T.A. Lipo, K. Byung-Il, "Material-Efficient Permanent-Magnet Shape for Torque Pulsation Minimization in SPM Motors for Automotive Applications," *IEEE Trans. Ind. Electron.*, vol. 61, pp. 5779-5787, 2014.
- [127] K.-C. Kim, "A Novel Method for Minimization of Cogging Torque and Torque Ripple for Interior Permanent Magnet Synchronous Motor," *IEEE Trans. Magn.*, vol. 50, pp. 793-796, 2014.
- [128] R. Lateb, N. Takorabet, F. Meibody-Tabar, "Effect of magnet segmentation on the cogging torque in surface-mounted permanent-magnet motors," *IEEE Trans. Magn.*, vol. 42, pp. 442-445, 2006.
- [129] M. Ashabani, Y.A.-R.I. Mohamed, "Multiobjective shape optimization of segmented pole permanent-magnet synchronous machines with improved torque characteristics," *IEEE Trans. Magn.*, vol. 47, pp. 795-804, 2011.
- [130] G.-H. Kang, Y.-D. Son, G.-T. Kim, J. Hur, "A Novel Cogging Torque Reduction Method for Interior-Type Permanent-Magnet Motor," *IEEE Trans. Ind. Appl.*, vol. 45, pp. 161-167, 2009.
- [131] W. Fei, Z.Q. Zhu, "Comparison of Cogging Torque Reduction in Permanent Magnet Brushless Machines by Conventional and Herringbone Skewing Techniques," *IEEE Trans. Energy. Conver.*, vol. 28, pp 664-674, 2013.
- [132] S.E. Abdollahi, S. Vaez-Zadeh, "Reducing Cogging Torque in Flux Switching Motors With Segmented Rotor," *IEEE Trans. Magn.*, vol. 49, pp. 5304-5309, 2013.
- [133] L. Dosiek, P. Pillay, "Cogging torque reduction in permanent magnet machines," *IEEE Trans. Ind. Appl.*, vol. 43, pp 1565-1571, 2007.
- [134] J. Hung, Z. Ding, "Design of currents to reduce torque ripple in brushless permanent magnet motors," *IET. Electr. Power. App.*, pp. 260-266, 1993.
- [135] H.-Y. Yang, Y.-C. Lim, H.-C. Kim, "Acoustic Noise/Vibration Reduction of a Single-Phase SRM Using Skewed Stator and Rotor," *IEEE Trans. Ind. Electron.*, vol. 60, pp. 4292-4300, 2013.
- [136] J.-P. Hong, K.-H. Ha, J. Lee, "Stator pole and yoke design for vibration reduction of switched reluctance motor," *IEEE Trans. Magn.*, vol. 38, pp. 929-932, 2002.
- [137] S.S.R. Bonthu, M.T.B. Tarek, S. Choi, "Optimal Torque Ripple Reduction Technique for Outer Rotor Permanent Magnet Synchronous Reluctance Motors," *IEEE Trans. Energy. Conver.*, vol. 33, pp 1184-1192, 2018.
- [138] D. Cameron, J. Lang, S. Umans, "The origin of acoustic noise in variable-reluctance motors," *IEEE IAS*, pp. 108-115, 1989.
- [139] H. Zhu, G. Zhou, J. Chen, H. Liu, "Analysis and study of skewed slot tooth distance on low electromagnetic noise of three-phase induction motor with squirrel cage rotor," *ICEF*, pp. 1-4, 2012.
- [140] C. Pollock, C.-Y. Wu, "Acoustic noise cancellation techniques for switched reluctance drives," *IEEE Trans. Ind. Appl.*, vol. 33, pp. 477-484, 1997.
- [141] Z.Q. Zhu, X. Liu, Z. Pan, "Analytical Model for Predicting Maximum Reduction Levels of Vibration and Noise in Switched Reluctance Machine by Active Vibration Cancellation," *IEEE Trans. Energy. Conver.*, vol. 26, pp. 36-45, 2011.
- [142] X. Liu, Z. Zhu, M. Hasegawa, A. Pride, R. Deodhar, T. Maruyama, Z. Chen, "Dc-link capacitance requirement and noise and vibration reduction in 6/4 switched reluctance machine with sinusoidal bipolar excitation," *2011 IEEE ECCE*, pp. 1596-1603, 2011.
- [143] Y.-S. Choi, H.H. Choi, J.-W. Jung, "Feedback Linearization Direct Torque Control With Reduced Torque

- and Flux Ripples for IPMSM Drives,” *IEEE Trans. Power. Electr.*, vol. 31, pp 3728-3737, 2016.
- [144] A. Hofmann, A. Al-Dajani, M. Bösing, R.W. De Doncker, “Direct instantaneous force control: A method to eliminate mode-0-borne noise in switched reluctance machines,” *IEMDC.*, pp. 1009-1016, 2013.
- [145] M. Divandari, A. Dadpour, “Radial force and torque ripple optimization for acoustic noise reduction of SRM drives via fuzzy logic control,” *INDUSCON.*, pp. 1-6, 2010.
- [146] P. Chen, T. Chen, J. Liang, B. Fahimi, M. Moallem, “Torque Ripple Mitigation Via Optimized Current Profiling in Interior Permanent Magnet Synchronous Motors,” *IEMDC.*, pp. 240-247, 2019.
- [147] F. Scuiller, “Third harmonic current injection to reduce the pulsating torque of a five-phase spm machine,” *IECON*, pp. 811-816, 2015.
- [148] C. Ma, L. Qu, R. Mitra, P. Pramod, R. Islam, “Vibration and torque ripple reduction of switched reluctance motors through current profile optimization,” *IEEE IEPC.*, pp. 3279-3285, 2016.
- [149] M. Takiguchi, H. Sugimoto, N. Kurihara, A. Chiba, “Acoustic Noise and Vibration Reduction of SRM by Elimination of Third Harmonic Component in Sum of Radial Forces,” *IEEE Trans. Energy. Conver.*, vol. 30, pp. 883-891, 2015.
- [150] N. Kurihara, J. Bayless, A. Chiba, “Noise and vibration reduction of switched reluctance motor with novel simplified current waveform to reduce force sum variation,” *IEEE IEMDC.*, pp. 1794-1800, 2015.
- [151] B. El Badsì, B. Bouzidi, A. Masmoudi, “Bus-clamping-based DTC: An attempt to reduce harmonic distortion and switching losses,” *IEEE Trans. Ind. Electron.*, vol. 60, pp 873-884, 2012.
- [152] M. Liu, F. Gu, Y. Zhang, “Ride Comfort Optimization of In-Wheel-Motor Electric Vehicles with In-Wheel Vibration Absorbers,” *Energies*, vol. 10, no. 10, pp 1647, 2017.
- [153] Yechen Qin, Ze Zhao, Zhenfeng Wang, Guofa Li, “Study of Longitudinal-vertical Dynamics for In-wheel Motor-driven Electric Vehicles,” *Automotive Innovation*, 2021.
- [154] M. Sunwoo, K.C. Cheok, N. Huang, “Model reference adaptive control for vehicle active suspension systems,” *IEEE Trans. Ind. Electron.*, vol. 38, pp. 217-222, 1991.
- [155] X. Shao, F. Naghdy, H. Du, H. Li, “Output feedback  $H_\infty$  control for active suspension of in-wheel motor driven electric vehicle with control faults and input delay,” *ISA Trans.*, vol. 92, pp. 94-108, 2019.
- [156] J.C. Tudón-Martínez, R. Morales-Menéndez, R. Ramírez-Mendoza, O. Sename, L. Dugard, “Comparison between a Model-free and Model-based Controller of an Automotive Semi-active Suspension System,” *IFAC Proceedings Volumes*, vol. 46, pp. 869-874, 2013.
- [157] W. Sun, H. Pan, Y. Zhang, et al., “Multi-objective control for uncertain nonlinear active suspension systems,” *Mechatronics*, vol. 24, pp 318-327, 2014.
- [158] Z. Liang, J. Zhao, Z. Dong, et al., “Torque Vectoring and Rear-Wheel-Steering Control for Vehicle’s Uncertain Slips on Soft and Slope Terrain Using Sliding Mode Algorithm,” *IEEE Trans. Veh. Technol.*, vol. 69, no. 4, pp. 3805-3815, 2020.